Received: 1 December 2023 | Revised: 18 June 2024 | Accepted: 21 June 2024

DOI: 10.1002/ajpa.24995

RESEARCH ARTICLE

AMERICAN JOURNAL OF BIOLOGICAL ANTHROPOLOGY
The Official Journal of the American Association of Biological Anthropologists

WILEY

Dental topography of prosimian premolars predicts diet: A comparison in premolar and molar dietary classification accuracies

Dorien de Vries[1,2] | Julie M. Winchester[3] | Ethan L. Fulwood[4] | Elizabeth M. St. Clair[5] | Doug M. Boyer[3]

[1]School of Science, Engineering, and Environment, University of Salford, Salford, UK

[2]Interdepartmental Doctoral Program in Anthropological Sciences, Stony Brook University, Stony Brook, New York, USA

[3]Department of Evolutionary Anthropology, Duke University, Durham, North Carolina, USA

[4]DeBusk College of Osteopathic Medicine, Lincoln Memorial University, Harrogate, Tennessee, USA

[5]University of Central Lancashire, Preston, UK

Correspondence
Dorien de Vries, School of Science, Engineering, and Environment, University of Salford, Salford, UK.
Email: d.devries@salford.ac.uk

Funding information
Directorate for Biological Sciences, Grant/Award Numbers: BCS-1304045, BCS-1552848, DBI-1759839; Natural Environment Research Council, Grant/Award Number: NE/T000341/1

Abstract

Objectives: This study tests whether (1) premolar topography of extant "prosimians" (strepsirrhines and tarsiers) successfully predicts diet and (2) whether the combination of molar and premolar topography yields higher classification accuracy than using either tooth position in isolation.

Materials and Methods: Dental topographic metrics (ariaDNE, relief index, and orientation patch count rotated) were calculated for 118 individual matched-pairs of mandibular fourth premolars (P_4) and second molars (M_2). The sample represents 7 families and 22 genera. Tooth variables were analyzed in isolation (P_4 only; M_2 only), together (P_4 and M_2), and combined (PC1 scores of bivariate principal component analyses of P_4 and M_2 for each metric). Discriminant function analyses were conducted with and without a measure of size (two-dimensional surface area).

Results: When using topography only, "prosimian" P_4 shape predicts diet with a success rate that is slightly higher than that of M_2 shape. When absolute size is included, premolars and molars perform comparably well. Including both premolar and molar topography (separately or combined) improves classification accuracy for every analysis beyond considering either in isolation. Classification accuracy is highest when premolar and molar topography and size are included.

Discussion: Our findings indicate that molar teeth incompletely summarize the functional requirements of oral food breakdown for a given diet, and that the mechanism selecting for premolar form is more varied than what is expressed by molar teeth. Finally, our findings suggest that fossil P_4s (in isolation or with the M_2) can be used for meaningful dietary reconstruction of extinct primates.

KEYWORDS
dental shape, DFA, dietary reconstruction, strepsirrhines, tarsiers

1 | INTRODUCTION

Primate molar shape correlates strongly with diet (Boyer, 2008; Cooke, 2011; Kay, 1975; Winchester et al., 2014). Primates whose diet consists primarily of fruits or nuts usually have molars with blunt and low cusps for crushing and grinding these foods (Bunn et al., 2011; Butler, 2000; Kay, 1975). Primates that primarily eat leaves or insects tend to have molars with steeply sloped cusps and crests for slicing through the tough cellulose of leaves or puncturing the hard chitin of insect exoskeletons (Bunn et al., 2011; Kay, 1975; Seligsohn & Szalay, 1978).

Dental topographic methods are designed to quantify functional aspects of the shape of teeth (Berthaume et al., 2018, 2019a; Bunn et al., 2011; Cuozzo & Sauther, 2006; Evans et al., 2007; Evans & Jernvall, 2009; Guy et al., 2013; Kay, 1975, 1978; Strait, 1993a, 1993b; Tiphaine et al., 2013; Ungar & M'Kirera, 2003; Zuccotti et al., 1998). Previous studies using dental topographic variables to quantify tooth shape have been successful at distinguishing between different dietary categories in a wide range of vertebrate clades (rodents and carnivorans: Evans et al., 2007; saurians: Melstrom, 2017; crocodyliforms: Melstrom & Irmis, 2019; bats: Santana et al., 2011). Within primates, dental topographic methods have been applied to quantify adaptations of various primate clades or subgroups (e.g., "prosimians": Boyer, 2008; Bunn et al., 2011; catarrhines: Lazzari & Guy, 2014; cercopithecoids: Avià et al., 2022; Bunn & Ungar, 2009; hominoids: Berthaume & Schroer, 2017; M'Kirera & Ungar, 2003; Pampush et al., 2022; platyrrhines: Allen et al., 2015; De Vries et al., 2024; Ungar et al., 2018; Winchester et al., 2014). These methods have also been used to answer numerous questions about the functional morphology and evolution of primates: for example, exploring the effects of tooth wear on functional morphology (Dennis et al., 2004; Pampush et al., 2016b; Ungar & Williamson, 2000), quantifying dietary niche contraction through time (Godfrey et al., 2012), and testing possible dietary competition between two Paleocene mammalian clades (Prufrock et al., 2016).

Because of demonstrated success in distinguishing different dietary categories in samples of extant species, dental topographic methods have been used to reconstruct the diets of extinct primates (Berthaume et al., 2018; Berthaume & Schroer, 2017; Boyer et al., 2010; Fulwood et al., 2021; Li et al., 2020; Morse et al., 2023; Seiffert et al., 2010, 2015, 2018; Selig et al., 2021, 2021b; Ungar, 2004). For paleodietary reconstruction, it can be important to carefully choose a comparative extant sample that is both closely related to, as well as morphologically and (potentially) ecologically analogous to the fossil species to be reconstructed, as Winchester et al. (2014) show that different primate clades can display different quantified morphological shape attributes even for similar diets. Extant "prosimian" (while "prosimian" is not a monophyletic clade, including strepsirrhines and tarsiers but no other haplorhines, we use this term to abbreviate "strepsirrhines and tarsiers") dental topography has been used to reconstruct early fossil primate diets such as Eocene adapiforms (Seiffert et al., 2015, 2018) and the enigmatic late Eocene primate *Nosmips* (Seiffert et al., 2010) based on their similar dental shapes. In contrast, to reconstruct the diets of Oligocene fossil anthropoids, Morse et al. (2023) used a combined sample of extant platyrrhines and prosimians.

Primate dental topographic studies usually focus on the lower second molar (M_2), and this tooth position has been shown to be able to characterize dietary adaptations with classification accuracies ranging from for example, 81.0% (Winchester et al., 2014) to 93.6% (extant prosimian sample, Seiffert et al., 2015) using a combination of different topographic variables as well as a measure of tooth size. Various dental topographic variables have been introduced, such as relief index (or RFI, Boyer, 2008; M'Kirera & Ungar, 2003), which is the ratio between the 3D area of the crown to the 2D outline area and reflects the number and height of cusps, length of crests, and crown height of the tooth shape. Complexity, measured as orientation patch count (or OPC, Evans et al., 2007), later expanded upon to orientation patch count rotated (or OPCR, Evans & Jernvall, 2009), measures the number of patches of the crown surface that consist of contiguous areas that face in the same direction out of eight compass directions. Complexity reflects the number of features, or "tools," of a tooth crown for breaking down foods, such as cusps and crests. Curvature, measured as Dirichlet normal energy (or DNE, Bunn et al., 2011), later expanded upon to ariaDNE (Shan et al., 2019) and convex DNE (Pampush et al., 2022), measures the deviation of a surface from being planar and reflects how much a surface bends. To briefly summarize the different functional aspects measured by these three dental topographic variables: relief (RFI) and curvature (DNE) are mainly driven by the shape of features on a tooth, whereas complexity (OPCR) is mainly affected by the number of features on a tooth (Winchester, 2016a). Combinations of several dental topographic variables tend to yield higher classification accuracies than one topographic variable alone. Previous studies on the dental topography of prosimian M_2s have shown that: RFI differs significantly between four dietary groups: insectivores have the highest relief, followed sequentially by folivores, omnivores, and lastly frugivores (Boyer, 2008); omnivores and frugivores have significantly lower OPCR values than folivores and insectivores (Bunn et al., 2011); and DNE differs significantly between dietary categories, following a similar pattern to RFI (Bunn et al., 2011).

Classification of dietary categories from dental topography can be further improved by the inclusion of a variable reflecting the primate's body size (e.g., molar area or length; Allen et al., 2015; Boyer, 2008). The inclusion of a proxy of body size especially aids in distinguishing prosimian insectivores from folivores, as folivore and insectivore dental topography is similar due to shared dental adaptations such as high, sharp cusps and crests. Only small primates can subsist on a primarily insectivorous diet, with the largest insectivorous primate still being an order of magnitude smaller than the smallest folivorous primate (Kay, 1975). Including a measure of size thus increases dietary classification accuracy. Including an additional tooth position may also reveal a better discriminatory power between folivores and insectivores; whereas the masticatory requirements of leaves and chitin might be similar, the initial ingestion stages of leaves versus that of insects might require different functional demands, thus raising the

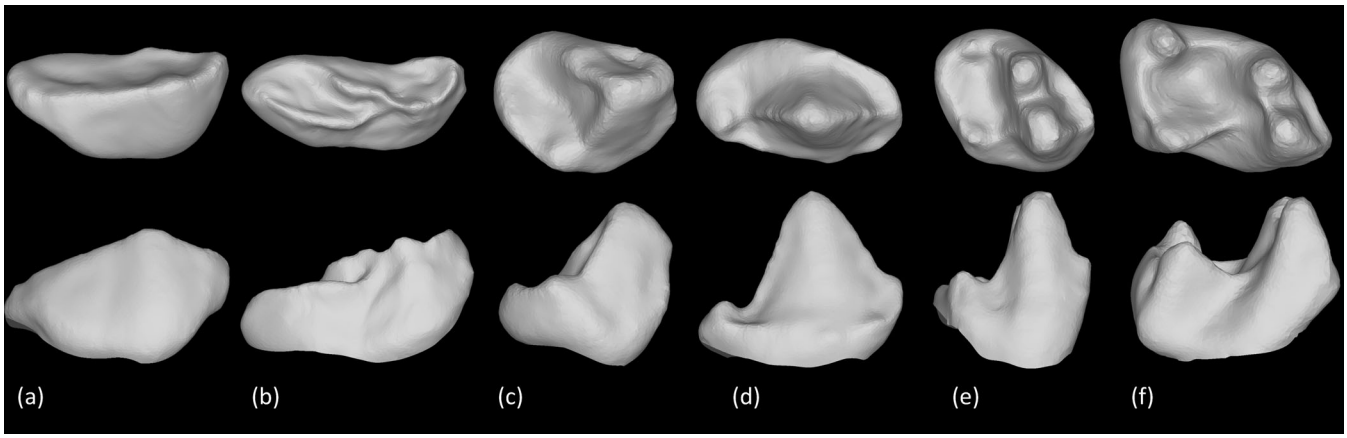

FIGURE 1 Premolar (P_4) shape variation of prosimians, not to scale. (a) Folivore *Indri indri* BMNH1981.719; (b) folivore *Avahi laniger* AMNH170501; (c) frugivore *Cheirogaleus medius* AMNH100654; (d) omnivore *Phaner furcifer* BMNH48.193; (e) insectivore *Loris tardigradus* AMNH217303; (f) insectivore *Galagoides demidovii* AMNH119810. Top row: occlusal view; bottom row: buccal view.

possibility of different, and possibly greater, dietary discrimination from premolars and molars.

Premolar topography has not received the same amount of attention in dietary prediction or reconstruction studies (although notable exceptions are Boyer et al., 2010; López-Torres et al., 2018; Scott et al., 2018; Seiffert et al., 2010; Selig & Silcox, 2022). This omission may be due to the varying function of premolars in feeding within primates (Selig & Silcox, 2022). Oral food processing is initiated with "ingestion" (Butler, 2000; Hiiemae & Crompton, 1985; Maier, 1984), during which the anterior teeth (incisors and canines, sometimes assisted by premolars), are used for the killing of prey, tearing of bark, opening of fruits, or scraping of resins. This is followed by mastication, in which food items are reduced in particle size and which can be divided into several stages. First, the puncture-crushing (or "fast close") stage is when the opposing dental arcades approach each other, wedging apart and crushing food. The subsequent "power stroke" (or "slow close") of mastication is performed by the posterior dentition (molars and sometimes premolars) and can further be divided into two phases: Phase I consists of crushing/shearing while the lower molar moves up and medially into centric occlusion; whereas Phase II consists of chewing/grinding as the lower molar continues moving medially and downward out of centric occlusion (Hiiemae & Kay, 1972; Hiiemae & Crompton, 1985; Kay, 1975; Kay & Hiiemae, 1974; or "grinding and crushing", Simpson, 1933). Phase I is thought to shear and crush food in smaller portions, whereas Phase II is thought to further grind segmented food particles down. Premolars can be used in ingestive and masticatory functions across primates.

The flexibility in premolar function is likely a result of their location in the toothrow (Selig & Silcox, 2022; Swindler, 2002), between the cutting and gripping incisors and canines on their mesial side, and the puncturing, crushing, and grinding molars on the distal side. The form and function of the premolars can also vary along the toothrow: in some primates the first premolar is more caniniform in shape and the last premolar (P_4) is at times more molariform in shape (Swindler, 2002). However, some primates may still use the last premolar for ingestion of food, such as exudativorous galagos and some lemurs which access and stimulate the flow of exudates by using their anterior dentition possibly assisted by premolars to gnaw and remove hardened exudate-plugs (Burrows et al., 2020; Selig & Silcox, 2022). For example, the tall, blade-like P_4 of *Phaner furcifer* (see Figure 1d) resembles a canine and may primarily act as one. Alternatively, some primate P_4 shape is more complex and molariform and these may functionally be more similar to molars. An extreme example of this is the P_4 of *Prolemur*, which has a diet consisting almost exclusively of bamboo, and has a distinctly molariform P_4 which is unique among Lemuridae (Seligsohn & Szalay, 1978; Swindler, 2002). Figure 1 and the figure guide in Data S1 provide examples of different premolar shapes in prosimians. Given this variation in form and function, we predict that adding information on premolar form should allow more precise and diagnostic predictions of the adaptive dietary habits for a species.

Using a large comparative sample of extant prosimians, this study assesses whether dental topography of the P_4 can successfully distinguish different diets. The aims of this study are to (1) assess the classification accuracy of P_4 topography in extant prosimians and (2) assess whether combining P_4 and M_2 topography of the same specimens improves classification accuracy over using either tooth position separately. This study also seeks to determine whether dental topography of a fossil primate P_4 could be used reliably for dietary reconstruction, and, if both a fossil P_4 and M_2 are available, whether combining topographic data of the P_4 and M_2 could improve dietary classification accuracy.

2 | MATERIALS AND METHODS

2.1 | Study sample

The study sample consists of the P_4 and M_2 of 118 prosimian toothrow specimens (236 teeth in total, all shared on MorphoSource, Boyer

et al., 2016, project ID 000552618) spanning 22 genera and 33 species (Tables S1 and S2 in Data S1). Every strepsirrhine and tarsier family is represented in our sample, except Daubentoniidae as this family lacks a P_4, with the following number of pairs of specimens per family: Tarsiidae 8, Lorisidae 31, Galagidae 10, Cheirogaleidae 21, Indriidae 9, Lemuridae 32, and Lepilemuridae 7. Each P_4 and M_2 pair originates from the same specimen and from the same side of the mandible. The majority of the M_2 specimens have previously been included in studies by Boyer (2008), Bunn et al. (2011), and Winchester et al. (2014). Compared to the samples used in those studies, this sample is supplemented with additional specimens to ensure dietary categories were represented as equally as possible.

2.2 | Data preparation

High-resolution plastic replica casts were created from molds of lower postcanine tooth rows using gray-pigmented EPOTEK 301 epoxy, and were scanned with a ScancoMedical brand µCT 40 machine (www.scanco.ch) at 10–18 µm resolution. The data captured by the µCT scanner was processed by the Scanco, Avizo (Visualization and Analysis) and Amira (Visage Imaging) software packages to produce three-dimensional models of tooth surfaces by manually setting the segmentation threshold for creating an isosurface. Using Amira, Avizo, and Geomagic software, the surface models of the postcanine tooth rows were cropped to extract the crown of the P_4 and, separately, that of the M_2. Tooth crowns were cropped along the base of the crown to include only the tooth crown and excluding any bone or root material. Minor deformations due to the molding process (e.g., small bubbles) were reconstructed using Geomagic software. Each specimen was manually oriented into occlusal view in the XY-plane, simplified to 10,000 triangles, and smoothed for 100 iterations in Avizo. Surfaces were checked to make sure no smoothing artifacts had appeared (as discussed by Spradley et al., 2017).

2.3 | Dental variables

The following variables were calculated using MorphoTester freeware (Winchester, 2016b) for the entire sample of P_4s and M_2s: 3D OPCR, 2D outline area (the two-dimensional surface area, or the "footprint," of the tooth), and 3D surface area (the surface area of the crown surface). Dental relief was measured using RFI (Boyer, 2008; Ungar & M'Kirera, 2003), which was calculated as the natural log of the square root of the surface area divided by the square root of the outline area (following Boyer, 2008). Curvature, or ariaDNE, was calculated in MATLAB (v2021b) (2021) using code provided by Shan et al. (2019).

Dental complexity was measured as 3D OPCR, with minimum faces of a patch set to three, and there being eight directional bins. The original version of this metric, OPC (Evans et al., 2007) is affected by the orientation of the surface file. OPCR (Evans & Jernvall, 2009), reduces the effects of this potential error using the average of eight rotations of 5.625°. Some notable limitations of OPCR are its vulnerability to large amounts of variation when comparing OPC/OPCR values between different studies (DeMers & Hunter, 2024) or different materials (casts versus original specimens, López-Torres et al., 2018). OPCR in isolation has been shown to have limited predictive power in some primate studies using the M_2 (e.g., 30% accuracy using a platyrrhine sample and 20.72% for a prosimian sample in Berthaume et al., 2019a; 44.1% accuracy using a platyrrhine sample and 38.8% for a prosimian sample in Winchester et al. (2014); but see de Vries et al. (2024) whose results show an accuracy of 68.5% for a platyrrhine sample, although the authors note that this is likely due to the different smoothing protocol they applied). This low predictive accuracy may indicate that primate molars have too small a variation in the number of features, or "tools," for the metric to hold a functional discriminative power. However, OPCR is able to detect some aspects of highly specialized morphology such as enamel crenulations in hard-object feeding platyrrhines (Winchester et al., 2014), and is relatively uncorrelated with other topographic metrics, which contrasts with curvature and relief that are often correlated (e.g., Winchester et al., 2014). OPCR thus provides a way of capturing features that may be missed by other dental topographic metrics. Additionally, P_4 OPC/OPCR has been shown to differ significantly across different degrees of molarization in fossil primates (OPC; Boyer et al., 2010 and 3D OPCR; Selig & Silcox, 2022), suggesting OPCR may be informative in quantifying premolar shape for distinguishing different dietary adaptations, especially as primate premolars appear to vary more in the number of features (i.e., ranging from sectorial to molariform) than primate molars do.

DNE is an algorithm that quantifies surface curvature (Bunn et al., 2011), and ariaDNE is a modification to and improvement on this algorithm (Shan et al., 2019). Both DNE and OPCR use the borders between triangles in their calculations. Therefore, DNE and OPCR values of the exact same specimen differ depending on the number of triangles selected when the specimen is down-sampled (Berthaume et al., 2019b; Shan et al., 2019). The metric ariaDNE differs from traditional DNE in its robusticity to mesh preparation differences (e.g., differences in triangle counts, smoothing protocols), as well as its lower sensitivity to mesh quality issues that can be introduced even during careful mesh preparation such as unequal triangle distribution or density, especially near mesh boundaries, than can cause "spikes" in DNE not related to the actual anatomical dental surface. Because of its lower sensitivity to these issues than conventional DNE, we chose to use ariaDNE in this study (Shan et al., 2019). AriaDNE was computed across a range of ε values, which determines the scale of features you want to be captured (ε set to 0.04, 0.06, 0.08, and 0.1, as recommended by Shan et al., 2019).

Conventional DNE has been expanded upon to distinguish between convex DNE and concave DNE (i.e., outwardly facing curvature versus inwardly facing curvature, respectively; Pampush et al., 2022). Convex DNE has been argued to reflect a clear functional signal better over conventional DNE, as Pampush et al. (2022) argue that convex DNE relates to features of the occlusal surface linked to shearing and cutting of food, whereas including concave DNE adds noise to the functional signal. This is shown to be particularly

important when considering hominoid molars, which have deep occlusal sulci that increase overall DNE, but, as they are concavely oriented, do not contribute to convex DNE. In contrast, conventional DNE and ariaDNE measure total-surface curvature, thus capturing various functions: the convex cutting edges for cutting or slicing, the shallow concave basins for gripping and crushing foods, and the steeper concave sulci that have unknown mechanical functions (see Pampush et al., 2022). We test whether ariaDNE, conventional DNE, and convex DNE differ in their dietary predictive power for our prosimian P_4 and M_2 sample and use the metric with highest classification accuracy. To do this, we calculated DNE and convex DNE using the R package molaR (v5.3; Pampush et al. 2016a, 2022). We thus use dental topographic metrics as discriminating shape variables for predicting different dietary categories.

Lastly, as a measure of tooth size the natural log of the 2D surface outline area was used, or "ln(OA)," either for the M_2 or for the P_4, depending on the analysis.

2.4 | Dietary categories

Dietary categories are shown in Table 1 and were assigned following the four-category classification scheme of Bunn et al. (2011), which is an updated version of the dietary schemes proposed by Boyer, 2008. This scheme is based on behavioral studies, gut contents, or fecal composition (see Boyer, 2008 for a more detailed explanation). The four categories are: folivore, frugivore, insectivore, and omnivore. Species for which insects or leaves make up over 50% of their diet (in most studies measured as time spent feeding rather than volume of food consumed), habitually or for at least 1–2 months a year, were classified as insectivores or folivores, respectively. Taxa for which fruit and/or seeds make up more than 50% of their diet, with only minor intake of insects or leaves, were considered frugivores. Taxa whose diet consist of fruits and either insects or leaves for roughly equal amounts throughout the year were classified as omnivores. Taxa were also considered omnivores when conflicting dietary preferences were reported in the literature.

The following species were assigned a dietary category to expand the published dietary classification scheme of Bunn et al. (2011): we classified *Microcebus murinus* as an omnivore based on varying dietary descriptions: Dammhahn and Kappeler (2008) report *M. murinus* as an omnivore with fruit being "a main component of the diet" for 24% (Dammhahn & Kappeler, 2008 tab. 6), but *M. murinus* is classified as a gumnivore or frugivore (depending on study period) by Thorén et al. (2011), and as a frugivore (63%) by Lahann (2007). *Nycticebus javanicus* was not assigned a dietary category by Bunn et al. (2011) based on a lack of published observational, gut content, or fecal data at the time of their publication. Rode-Margono et al. (2014) found that the greatest component of *N. javanicus*' diet was exudates (56%) followed by nectar (32%). According to Cabana et al. (Cabana et al., 2017 Table 1), *N. javanicus*' majority of crude protein intake was derived from insects. As this results in conflicting dietary categories (i.e., gumnivore or insectivore), *N. javanicus* was categorized as an omnivore. It is worth noting that no taxa were classified as gumnivores by Boyer (2008), and that *Phaner furcifer* was classified as an omnivore although it has a high percentage of exudates listed for its diet (65%, see Boyer, 2008 Table 1). We follow this classification scheme based on the assumption that gums and tree saps are not mechanically demanding during mastication, and we therefore do not include these foods to determine the dietary category, although we discuss below how some postcanine teeth can be used to access these foods during the ingestion phase. *Otolemur crassicaudatus* was assigned the omnivore category based on its diet consisting of fruits, insects, and exudates to varying degrees (Long et al., 2021 Table 2).

TABLE 1 Dietary classification scheme used in this study.

Taxon	Dietary category
Arctocebus calabarensis	Insectivore
Avahi laniger	Folivore
Carlito syrichta	Insectivore
Cephalopachus bancanus	Insectivore
Cheirogaleus spp.	Frugivore
Eulemur rufus	Omnivore
Galagoides demidovii	Insectivore
Galago senegalensis	Insectivore
Hapalemur griseus	Folivore
Indri indri	Folivore
Lemur catta	Omnivore
Lepilemur spp.	Folivore
Loris tardigradus	Insectivore
Microcebus spp.	Omnivore
Mirza coquereli	Omnivore
Nycticebus spp.	Omnivore
Otolemur crassicaudatus	Omnivore
Perodicticus potto	Frugivore
Phaner furcifer	Omnivore
Prolemur simus	Folivore
Propithecus spp.	Folivore
Sciurocheirus alleni	Omnivore
Tarsius spectrum	Insectivore
Varecia variegata	Frugivore

Note: We expanded the Bunn et al., (2011) classification scheme by assigning *Microcebus murinus*, *Nycticebus javanicus*, and *Otolemur crassicaudatus* to the "omnivore" dietary category (see text for more details).

2.5 | Statistical analyses

All analyses were run in R (v4.2.0, R Core Team, 2022). To obtain descriptive statistics per dietary group, the "var" and "mean" function from the base R package (v4.2.0, R Core Team, 2022) was run on specimen data, as well as natural log transformed species averaged

data to account for the different sized teeth and unequal sample sizes. To assess the correlation and its direction of a dental metric between the two tooth positions, we ran Pearson's *r*-tests for paired data using the "cor.test" function from the base R package (v4.2.0, R Core Team, 2022) for the total-sample as well as for each dietary group separately. The Pearson's product–moment correlation values of each dietary group were compared to the total-sample value testing for a significant difference using code from Field et al. (2012) that first transforms the Pearson's *r*-value to a *z*-score before calculating the *z*-difference score and the two-tailed *p*-value. To account for phylogeny, phylogenetic generalized linear models were also run using the "pgls" function from the R package caper (v1.0.1, Orme et al., 2018), a phylogeny downloaded from 10kTrees (selecting all strepsirrhine families and the Tarsiidae family and using the consensus tree, Arnold et al., 2010), and species averages for all data. One species was excluded from the phylogenetic analyses as it was not included in the phylogeny (*Tarsius spectrum*; although we note that *Cephalopachus bancanus* and *Carlito syrichta* remained included), resulting in a total of 32 species to be included. Correlations were considered as follows: an absolute *r*-value of 0–0.19 as very weak, 0.2–0.39 as weak, 0.40–0.59 as moderate, 0.6–0.79 as strong, and 0.8–1 as very strong. Note that these distinctions were chosen arbitrarily, and results are discussed in context.

To assess the effects of dietary categories on premolar dental topographic metrics, one-way ANOVAs were run using the "aov" function of the base R package (v4.2.0, R Core Team, 2022). Residuals from the ANOVA were checked to be normally distributed using a Shapiro–Wilk normality test using the "shapiro.test" function of the R package stats (v4.2.0, R Core Team, 2022). When residuals were non-normally distributed, a Kruskal–Wallis test was run using the "kruskal.test" function, also from the R package stats. When a significant difference was found between categories using the ANOVA, a Games–Howell post hoc test was applied using the "games_howell_test" function of the R package rstatix (v0.7.2 Kassambara, 2023). Games–Howell post hoc tests do not assume equal sample size or equal variance per sample and were therefore deemed appropriate for this study. When a significant difference was found using the Kruskal–Wallis test, a Dunn test with Bonferroni post hoc correction was run using the "dunn.test" function of the R package dunn.test (v1.3.5, Dinno & Dinno, 2017). To account for phylogeny, we also conducted phylogenetic ANOVAs in R using the "phylANOVA" function from the R package phytools (v1.5–1, Revell, 2012) and the same 10kTrees phylogeny as mentioned above.

To assess the ability of dental topographic variables to successfully predict the diet, with or without a measure of tooth size, we ran quadratic discriminant analyses (QDA) using the "qda" function of the R package MASS (v7.3-56, Ripley et al., 2013). We chose QDA as this analysis, unlike the more common linear discriminant analysis, does not assume equal variance of categories. Prior probabilities were set to reflect the sample sizes of the different diet groups by setting CV to "TRUE." To assess classification accuracy, the QDAs were run using a jack-knife approach (leave-one-out). Overall classification accuracy was calculated as the percentage of correctly classified specimens.

To assess whether combining topographic data of the P_4 with that of the M_2 yielded higher classification accuracy, two different methods were used. First, the topographic data of the P_4 and that of the M_2 were kept as separate factors in the QDA (e.g., diet $\sim$ RFI P_4 + OPCR P_4 + ariaDNE P_4 + RFI M_2 + OPCR M_2 + ariaDNE M_2). Second, the first principal component of a bivariate principal component analysis (PCA) of each variable was used (e.g., diet $\sim$ PC1 of bivariate PCA of P_4 and M_2 RFI + PC1 of bivariate PCA of P_4 and M_2 OPCR + PC1 of bivariate PCA of P_4 and M_2 ariaDNE) to test whether any increase in classification accuracy when P_4 and M_2 were included was driven by an increase in the number of variables or model complexity. The use of the bivariate principal components kept the number of variables consistent between single tooth locus-only analyses and analyses including P_4 and M_2 data.

3 | RESULTS

3.1 | Classification accuracy of dental topographic metrics in isolation

Values of conventional DNE (i.e., including both concave and convex curvature), convex DNE, and ariaDNE are comparable across all three curvature variables for the P_4 and the M_2 of different diets as shown in Figure 2. Classification accuracies across variables vary for the P_4, the M_2, as well as P_4 + M_2 (see Table 2), and classification accuracy differences between the different curvature variables are at the most 10.2%. In all tests, ariaDNE performs best and has the highest classification accuracy out of the different curvature metrics, and convex DNE has the lowest classification accuracy. Our results show that including concave DNE does not create a considerable amount of noise for our prosimian sample, and in fact appears to be informative for predicting diet, specifically for premolars (with P_4 ariaDNE having 10.2% higher classification accuracy than convex DNE, see Table 2) and expressed to a lesser degree for molars (with M_2 ariaDNE having a 4.2% higher classification accuracy than convex DNE, see Table 2). As ariaDNE evinced the highest predictive power for each tooth position, we use ariaDNE in the rest of the analyses. The results reported here only discuss ariaDNE values with ε set to 0.04, the lowest ε value of our study, thus picking up on small-scale features in dental shape. This ε value resulted in the highest classification accuracy compared with when ε was set to 0.06, 0.08, and 0.1 (capturing medium and larger-scale features). Raw values of these and all other metrics are included in the R code and input data (see Data Availability Statement).

OPCR shows higher dietary predictive power for P_4s than for M_2s (50% and 38.1%, respectively, see Table 2) whereas RFI performs comparatively well for the different tooth positions (P_4: 48.1%, M_2: 52.5%, see Table 2). Descriptive statistics of specimen values are listed in Table 3, and those of natural log transformed species averages in Table S3.

3.2 | Comparison and correlation between P_4 and M_2 dental variables

Average premolar and molar values of the total sample show that, compared to molars, premolars, on average, have less curvature (average P_4 ariaDNE is 88% of average M_2 ariaDNE); higher relief (113% of M_2 RFI); lower complexity (71% of M_2 OPCR); and are smaller (76% compared to M_2 ln (OA), see Table 3 for a breakdown per dietary category).

Correlation coefficients between different topographic metrics (r and p values) are listed in Table 4 and illustrated in Figure 3. When specimen values are considered, all dental metrics correlate positively between tooth-positions with $p < 0.01$: OPCR and RFI had weak to moderate correlations between tooth positions ($r = 0.39$ and $r = 0.46$, respectively), ariaDNE correlates strongly between tooth position ($r = 0.61$), and size shows the strongest correlation between premolars and molars ($r = 0.97$).

When phylogeny is taken into account and species averages are used, total-sample correlations change only slightly (see Table 4). All phylogenetically adjusted r values have $p \leq 0.05$ except for RFI ($p = 0.13$, see Table 4).

TABLE 2 Quadratic discriminant analyses classification accuracy calculated using leave-one-out approach shown in percentage for the different dental topographic metrics in isolation.

Variable	P_4	M_2	$P_4 + M_2$
ariaDNE	51.7%	54.2%	61.0%
DNE	45.8%	52.5%	52.5%
Convex DNE	41.5%	50.0%	50.9%
OPCR	50.0%	38.1%	47.8%
RFI	48.3%	52.5%	66.1%

Abbreviations: DNE, Dirichlet normal energy; OPCR, orientation patch count rotated; RFI, relief index.

Not all dietary categories follow the total-sample patterns in the strength of correlation between tooth positions. Insectivores differ significantly (with a two-tailed $p \leq 0.05$ for the z-difference) from the total-sample correlation for the three dental topographic metrics, as did omnivores for ariaDNE and OPCR. For these metrics, the omnivores and insectivores show a very weak correlation between P_4 and M_2 with r values between −0.09 and 0.15, suggesting the relationship between P_4 and M_2 function varies within these diets. This is in contrast with the weak to strong correlation exhibited by the total-sample or frugivore and folivore samples for the same dental metrics, suggesting the relationship between P_4s and M_2s is more uniform within these diets. Correlation in size between tooth positions is very strong for every dietary category, however, the r values of insectivores (0.85) and folivores (0.9) are significantly lower than the total-sample r value of 0.97 (with a two-tailed $p \leq 0.05$ for the z-difference). It should be noted that the r values for the omnivore-sample and insectivore-sample are estimated with p values >0.05 except for tooth size, whereas r values for frugivores and folivores are estimated with $p \leq 0.05$. See the Data S1 for a list of all r values, phylogenetically adjusted r values, and p values for each dental metric per dietary category.

3.3 | Premolar (P_4) topography per dietary group

All premolar topographic variables differ significantly between at least two dietary categories (see Figure 4 and Table S4 in Data S1). Figure 5 shows the representative premolar shape per dietary group based on the P_4 specimen that exhibited the ariaDNE value closest to the mean value of that dietary group. P_4 ariaDNE is significantly higher for insectivores and folivores than that of omnivores and frugivores; P_4 RFI is significantly lower for folivores compared to all other diets, and insectivores have significantly higher P_4 RFI than omnivores do; P_4 OPCR is significantly higher for premolars of folivores than those of all other diets (albeit with high variance for every category, see

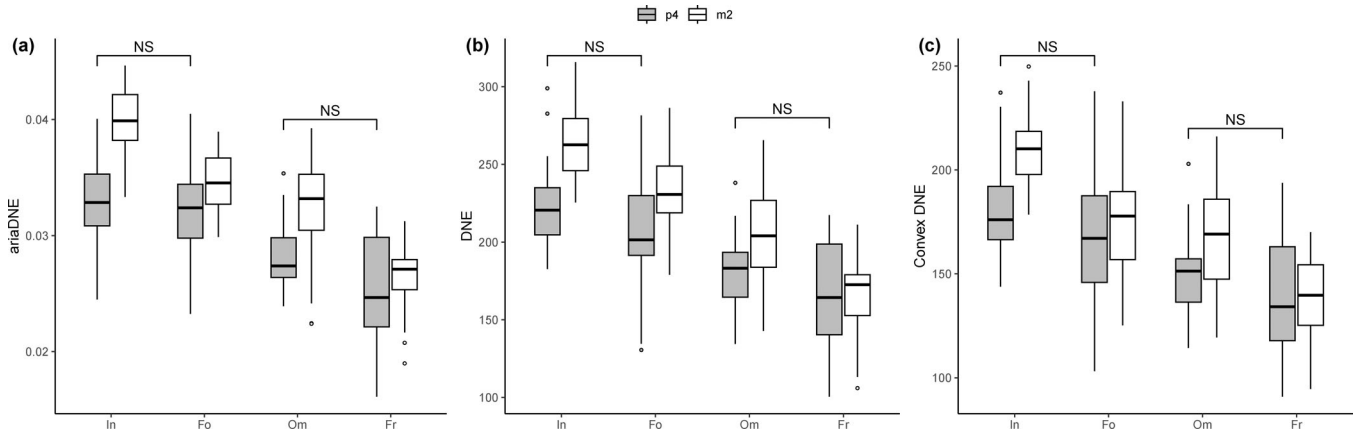

FIGURE 2 Dental curvature measured as different dental curvature metrics for this study's "prosimian" sample: (a) ariaDNE, (b) Dirichlet normal energy (DNE), and (c) convex DNE. All pairwise comparisons in the ANOVA between P_4 topographies are significant ($p < 0.05$) except for those indicated as not significant with "NS." Pairwise comparisons for the M_2 topographical data are not marked as significant or nonsignificant (See Data S1 for this). Fo, folivores; Fr, frugivores; In, insectivores; Om, omnivores.

TABLE 3 Descriptive statistics for premolar and molar specimen values for RFI, OPCR, ariaDNE ($\varepsilon = 0.04$), and the natural log of outline area by dietary category following the dietary scheme of Bunn et al. (2011).

Variable	Diet	*N*	P_4 mean (% compared to M_2)	P_4 variance	M_2 mean	M_2 variance
ariaDNE	Folivore	32	0.032 (91%)	1.5e-5	0.035	6.6e-6
	Frugivore	20	0.025 (96%)	2.3e-5	0.026	1.1e-5
	Insectivore	25	0.033 (83%)	1.2e-5	0.040	8.7e-6
	Omnivore	41	0.028 (88%)	7.1e-6	0.032	1.7e-5
	Total	**118**	**0.030 (88%)**	**2.2e-5**	**0.034**	**3.2e-5**
RFI	Folivore	32	0.48 (104%)	2.3e-3	0.46	1.8e-3
	Frugivore	20	0.54 (126%)	4.0e-3	0.43	3.8e-3
	Insectivore	25	0.58 (107%)	1.3e-3	0.54	8.8e-4
	Omnivore	41	0.55 (117%)	1.7e-3	0.47	1.3e-3
	Total	**118**	**0.54 (113%)**	**3.6e-3**	**0.48**	**3.3e-3**
OPCR	Folivore	32	64 (81%)	288	79	174
	Frugivore	20	48 (62%)	179	78	171
	Insectivore	25	50 (68%)	122	73	38
	Omnivore	41	47 (68%)	65	69	74
	Total	**118**	**53 (72%)**	**206**	**74**	**123**
ln (outline area)	Folivore	32	2.53 (87%)	0.40	2.9	0.30
	Frugivore	20	1.99 (80%)	0.78	2.5	0.48
	Insectivore	25	0.99 (58%)	0.09	1.7	0.13
	Omnivore	41	1.27 (71%)	0.88	1.8	0.61
	Total	**118**	**1.67 (76%)**	**0.92**	**2.19**	**0.63**

Note: Total sample values are shown in bold.
Abbreviations: DNE, Dirichlet normal energy; OPCR, orientation patch count rotated; RFI, relief index.

TABLE 4 Correlation in dental metrics between the P_4 and M_2 as *r* (calculated using specimen values of 118 pairs of specimens) and phylogenetically adjusted *r* (calculated using specimen means of 32 species).

	r	*p*	*t* (df)	Phylogenetically adjusted *r*	*p*	*F* (df)
ariaDNE	0.61	<0.01	8.31 (116)	0.65 ($\lambda = 0.62$)	<0.01	23.94 (30)
RFI	0.46	<0.01	5.6 (116)	0.21 ($\lambda = 0.55$)	0.13	2.44 (30)
OPCR	0.39	<0.01	4.5 (116)	0.4 ($\lambda = 0.51$)	0.01	6.93 (30)
ln (outline area)	0.97	<0.01	43.9 (116)	0.97 ($\kappa = 0$)	<0.01	441.1 (30)

Abbreviations: DNE, Dirichlet normal energy; OPCR, orientation patch count rotated; RFI, relief index.

Table 3); and average P_4 size increases across dietary categories as follows: insectivores < omnivores < frugivores < folivores, with insectivore and omnivore P_4s being significantly smaller than those of frugivores and folivores.

The phylogenetic ANOVAs result in a significant difference in P_4 dental topography between dietary categories only for ariaDNE and RFI. Phylogenetically adjusted premolar ariaDNE differs significantly between dietary categories with $p = 0.02$ ($n = 32$ species, $F = 10.12$), and the post hoc test shows that this is due to significant differences between ariaDNE of folivores and frugivores (simulation-based $p = 0.03$) and that of insectivores and frugivores ($p = 0.02$). Phylogenetically adjusted RFI also differs significantly between diets with a simulation based *p*-value of 0.04 ($n = 32$ species, $F = 8.89$), however, the pairwise corrected *p*-values of the post hoc test do not yield a *p* value ≤0.05.

See the Data S1 for M_2 ANOVA, Kruskal–Wallis, Games–Howell, and Dunn test post hoc test results.

3.4 | Classification accuracies

Premolar topography only (thus excluding a measure of size) performs slightly better than molar topography: 67.8% accuracy versus 61.9% accuracy, respectively (see Table 5). When looking at the breakdown of the QDA results per dietary group (see Table S5 in Data S1), the main difference to note is that P_4 QDA results indicate particular challenges for classifying frugivores based on topography alone (with only 30% accuracy) while classifying folivores with a high accuracy (72%), whereas the M_2 QDA classifies frugivores without much error (70% accurate) and instead struggles to accurately classify folivores (34%).

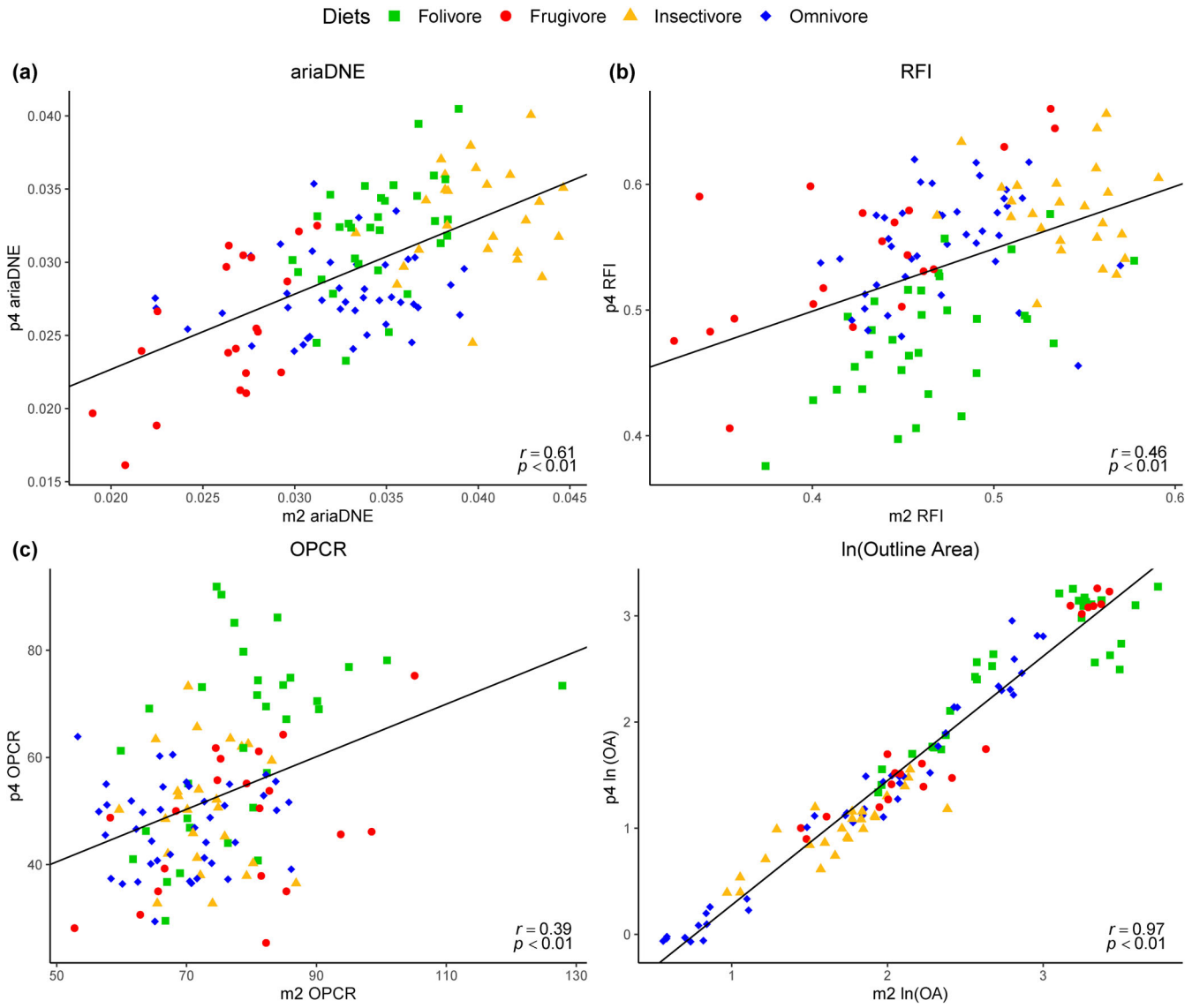

FIGURE 3 Correlation of dental topographic variables (a) ariaDNE; (b) relief index (RFI); (c) orientation patch count rotated (OPCR); and (d) natural log of outline area between P_4 and M_2 of the same specimen. Strength of total-sample correlation is listed as the *r* and *p*-value in bottom right of each plot. See Data S1 for correlation values and regression lines per dietary group.

Combined topography improves classification accuracy with an average of 6% (3.4% and 9.3% improvement for P_4 and M_2, respectively; see Table S6 in Data S1 for a breakdown of variance captured by PC1 of each PCA). Classification accuracy improves even more when premolar and molar topography are included as separate variables with an average improvement of 13.2% (10.2% and 16.1% improvement for P_4 and M_2, respectively). In both cases, the QDA of combined premolar and molar topography show much more evenly distributed classification accuracies between different diets (all ≥50%) than when P_4 and M_2 are analyzed separately.

When a measure of size is included in the QDA, premolar topography and premolar size perform similarly successfully to molar topography and molar size with classification accuracy difference being only 2.6%. P_4 QDA results indicate that even when including size, frugivores are still classified with the lowest accuracy (40%), in contrast, the low classification accuracy of M_2 topography only for folivores disappears when including a measure of size and folivore accuracy increases from 34% to 72% (see Table S5 in Data S1). Including size results in classification accuracy improving in all cases with an average of 6.1% compared to the same analysis without size (ranging from 0% to 12.7% from). When combined topography and size is used, classification accuracy is similar to that of separate premolar + size or molar + size variables with only 0.8% difference.

4 | DISCUSSION

4.1 | Dental topographic variance of premolars versus molars

Even though premolars are thought to be more variable in form and function compared to molars, this is only partially supported by the

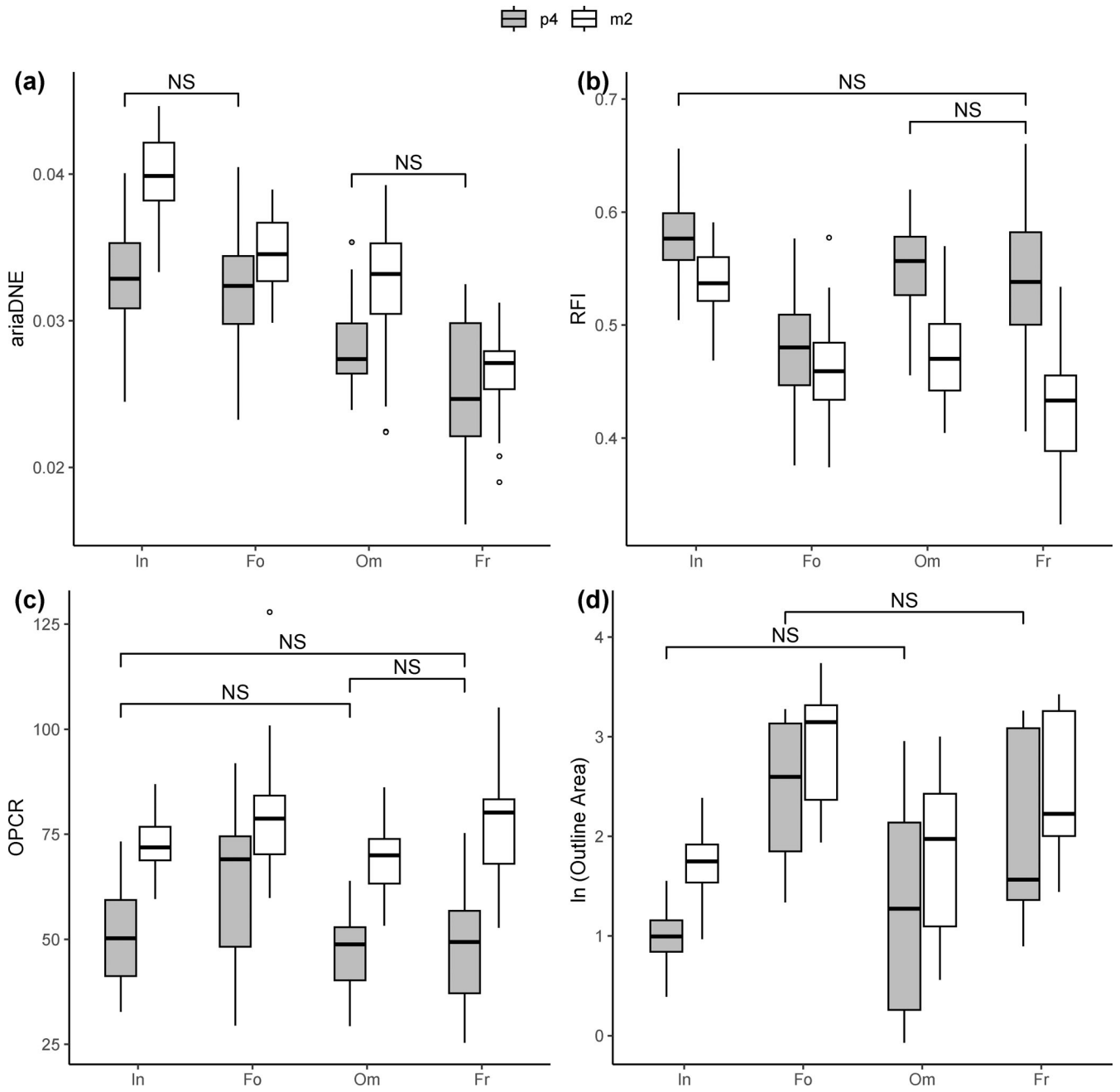

FIGURE 4 Boxplots of dental topographic variables (a) ariaDNE; (b) relief index (RFI); (c) orientation patch count rotated (OPCR); and (d) natural log of outline area of P_4 (gray) and M_2 (white) per dietary category. All pairwise comparisons in the ANOVA between P_4 topographies are significant ($p < 0.05$) except for those indicated as not significant with "NS." Phylogenetic ANOVA results differed and are mentioned in the main text. Pairwise comparisons for the M_2 topographies are not marked as significant or nonsignificant; see Data S1 for a list of these *p*-values. Fo, folivores; Fr, frugivores; In, insectivores; Om, omnivores.

dental topography (see Table 3 and S3 in Data S1) of our sample of molded, cast, scanned, and digitally reconstructed prosimian teeth. In fact, total sample RFI and ariaDNE (calculated from natural log transformed species averages data to account for the different sized teeth and unequal sample sizes, see Table S3 in Data S1) have greater variance for M_2s than P_4s. OPCR, in contrast, shows considerably greater variance for premolars than for molars, with premolars having 3.25 times the variance in OPCR than molars do. OPCR is mainly affected by the number of "tools" on a tooth, such as cusps, ridges, cingulae (Winchester et al., 2014), and thus supports that premolars have a greater variance in the number of "tools" than molars do. Counterintuitively, our results show that despite a greater variety in premolar OPCR, the curvature, or ariaDNE, of the premolar is actually slightly less varied in premolars than it is in molars. Finally, 2D tooth size also has a greater variance in premolars than in molars, but only slightly so. As RFI has a lower degree of variance in premolars

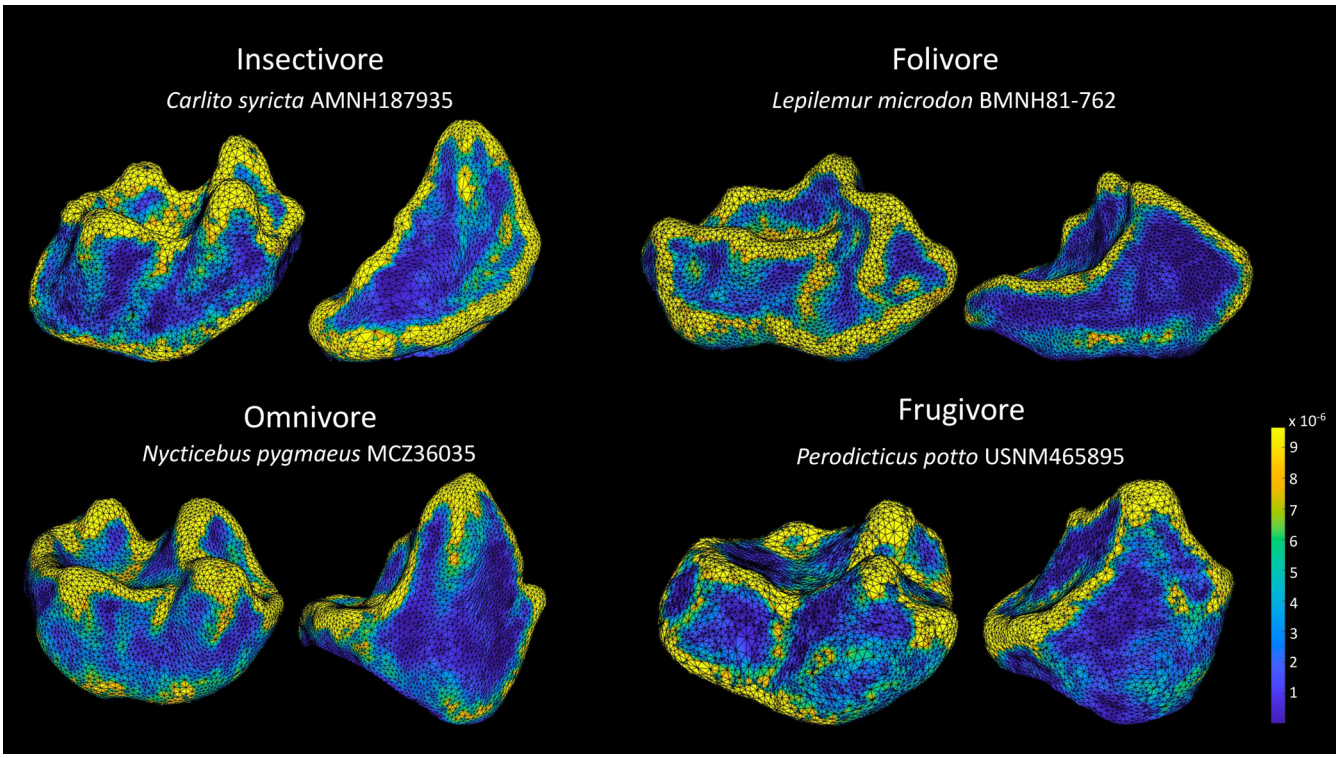

FIGURE 5 Representative P_4 shape and ariaDNE per dietary group based on the specimen's P_4 ariaDNE value being closest to the mean for the diet. M_2s of the same specimen are shown for comparison (M_2 left, P_4 right). Not to scale. *Carlito syrichta* AMNH187935 P_4 ariaDNE: 0.0325; *Lepilemur microdon* BMNH81-762 P_4 ariaDNE: 0.0318; *Nycticebus pygmaeus* MCZ36035 P_4 ariaDNE: 0.0282; and *Perodicticus potto* USNM465895 P_4 ariaDNE: 0.0252.

than it does in molars, this indicates that, despite 2D size being more variable in premolars than in molars, the three-dimensional surface area of premolars scales with outline area in a more constrained way (i.e., resulting in a less varied RFI) than molars do.

4.2 | Premolar and molar adaptations to different diets

Premolar topography is significantly correlated with molar topography for all variables, ranging from being weak (OPCR), to moderate (RFI), strong (ariaDNE), and very strong (size) in correlation. However, there is a lot of scatter in these relationships suggesting that both tooth positions can help independently explain variance in diet as shown by the classification results having strikingly different accuracies per dietary group between tooth positions (see above).

The complementing power of premolar topography when predicting diet is exhibited by its unanimous improvement in classification accuracy when combining P_4 and M_2 topography. Misclassifications in the QDA model of premolar topography is driven by confusion between frugivores and omnivores, with 45% of frugivores being classified as omnivores (see Table S5 in Data S1). Frugivores and omnivores share a relatively blunt premolar shape that lacks sharp ridges and cusps, differing from the low-crowned but sharply ridged folivore P_4s and the high-crowned and sharp insectivore P_4s. In contrast, it is the folivore M_2s that are misclassified on molar topography alone, predominantly as omnivores (with 53% of folivores being classified as omnivores, see Table S5 in Data S1). Folivore and omnivore molars share a low crown relief with a relatively high sharpness. Omnivore and frugivore M_2s are classified with high accuracy, driven by variation in crown height and bluntness, which is exceptionally low for frugivores and relatively moderate for omnivores that do exhibit some sharper and higher features in their M_2 shape. Although folivore molars exhibit a distinct set of features like their sharp and in some taxa low ridges (like *Avahi* and *Indri*), topographic metrics do not consistently distinguish these from the high columnar cusps of insectivores or the low crowns of frugivores. Thus, including topography of P_4s improves the classification accuracy of folivores while including M_2 topography improves the classification of frugivores compared with QDA results of P_4 or M_2 topography alone.

Folivores exhibit a unique pattern in how P_4 and M_2 complement each other in RFI and OPCR compared with other diets. Whereas omnivores and frugivores, and insectivores to a lesser extent, have considerably higher relief in their P_4 than in their M_2, folivores typically have P_4 RFI that is nearly as low as that of its M_2. These results quantify the qualitative pattern of P_4s of frugivores, omnivores, and some insectivores being more caniniform, simple, and columnar in shape (see Figure 5), while the P_4s of folivores is shaped as a sharp but low, blade-like tooth. Folivore OPCR is unique in a greater similarity in premolar and molar values: whereas frugivores, omnivores, and

TABLE 5 Classification accuracies of the quadratic discriminant analyses.

Dental topography	Accuracy
P_4 topography	67.8%
M_2 topography	61.9%
Combined P_4 and M_2 topography (PCA $P_4 + M_2$)	71.2%
Separate P_4 and M_2 topography ($P_4 + M_2$)	78.0%
Dental topography + size	
P_4 topography + P_4 size	72.0%
M_2 topography + M_2 size	74.6%
Combined P_4 and M_2 topography + size (PCA $P_4 + M_2$)	78.8%
Separate P_4 and M_2 topography + size ($P_4 + M_2$)	78.0%

Note: P_4 topography = P_4 ariaDNE, P_4 RFI, and P_4 OPCR. P_4 size = ln(P_4 outline area). M_2 topography = M_2 DNE, M_2 RFI, and M_2 OPCR. M_2 size = ln(M_2 outline area). See text for a detailed explanation of combined variables using principal component analysis (PCA) scores.

insectivores exhibit a consistent pattern of having considerably lower P_4 OPCR than that of their M_2s, folivore exhibit high average P_4 complexity that is nearly as high as that of its M_2s. This quantifies the qualitative pattern of folivores having distinctly complex P_4s that have ridges and cusps creating basins and shelves (or "patches"). This pattern is most extreme in the molariform P_4s of *Hapalemur* (see the Data S1 for a figure guide of every genus included in the study sample) but is also present in the P_4 of folivore *Lepilemur* (Figure 5). Folivores thus appear distinct from other dietary groups in having P_4s that are more topographically similar to their M_2s. Most representatives of other diets demonstrate a consistent pattern of typically more columnar, higher crowned, and simpler P_4s with fewer cusps and ridges than their M_2s (although some insectivores are an exception, e.g., *Galago* and *Galagoides*). When extrapolating these findings to the framework of a puncture-crushing (or fast close) stage and a power stroke (or slow close) stage, with power stroke Phase I (crushing/shearing) and Phase II (grinding), we suggest these shape results indicate that (1) the P_4s of frugivores, omnivores, and (some) insectivores appear primarily adapted for puncture-crushing and (2) folivore P_4s, besides functioning during puncture-crushing, have also been recruited to contribute to the power stroke, and that their P_4s therefore exhibit more adaptations for both Phase I and Phase II actions such as shearing and grinding already broken-up food particles into even smaller particles, preparing particles for digestion.

Lastly, dental adaptations for exudativory were not specifically tested for in our study. The only obligate exudate feeder taxa in our sample are *Nycticebus* spp., *Otolemur crassicaudatus*, and *Phaner furcifer*. *Nycticebus* is reportedly accessing exudates by "*de novo* gouging" using its anterior dentition only for gouging an opening in the tree bark (category 2 in Burrows et al., 2020). *Otolemur* and possibly *Phaner* access tree gums by using their anterior dentition and possibly their premolars to gnaw and twist away semi-dried exudate-plugs (category 3 in Burrows et al., 2020). The exudate feeders in our sample, *Nycticebus*, *Otolemur*, and *Phaner*, possess a high, columnar cusp on their P_4 seemingly ideal for puncturing (see figures in Data S1). The P_4 of *Nycticebus* and *Phaner* is simpler and caniniform in its appearance, while the P_4 of *Otolemur* is more complex and somewhat "molariform" in having additional cusps distally located (resulting in higher topographic values, especially RFI, compared with average *Nycticebus* and *Phaner* topography), albeit in no way similar in shape or topography to the lower crowned, molariform P_4s of *Prolemur* and *Hapalemur*. Based on our very limited exudativorous sample of three taxa, we do not find a distinct pattern in premolar shape and topography consistent with the different exudate-accessing categories presented in Burrows et al. (2020).

4.3 | Classification accuracy of premolars, molars, and the combination of both

QDA models using prosimian premolar dental topography and size are able to predict diet with a similar accuracy as models using molar dental topography and size. Despite the different functional roles of premolars among the taxa in our sample, or possibly because of this, premolar topography reflects different diets and the diets' processing requirements in a consistent way and can therefore be used to confidently quantify and predict dietary adaptations. However, when a measure of size is excluded, premolars slightly outperform molars in dietary classification accuracy. Based on our results, we deem these results to be similar enough between tooth positions to conclude that both tooth positions reflect the processing requirements of diets similarly well, and both tooth positions' shapes predict diet with similar accuracy. A notable difference in predictive power of dental topographic metrics in isolation is the classification accuracy of OPCR of premolars versus that of molars: whereas OPCR does not distinguish between dietary adaptations in prosimian molar shape very well and has the lowest predictive power of the tested dental topographic metrics by ~12%–14%, it performs well in distinguishing between different dietary groups using premolars. We interpret the difference in predictive power of OPCR to support that premolars have the necessary variation in the number of features or "tools" (i.e., ranging from sectorial to molariform) needed for OPCR values to differ sufficiently to have dietary predictive power, and vice versa, that the variation in the number of prosimian molar features is too small to have meaningful differences in OPCR between different dietary adaptations. We note again that even for premolars, OPCR values have great variance and that it is mostly informative for separating folivores with high OPCR values from the other three dietary categories that, on average, have lower OPCR values.

Combined topography of premolars and molars is highly accurate in distinguishing dietary categories of prosimians. When size is included, the differing predictive powers of keeping premolar and molar metrics separate versus combining in PCAs, is minimal (0.8%). This shows that when keeping the number of parameters constant, we still find a considerable increase in classification accuracy when combining both premolar and molar topography compared to including either one of the two. Both premolars and molars have the same number of significant and insignificant pairwise comparisons. However, they differ in which specific comparisons are significant. For example, whereas RFI does not differ significantly between folivore

and omnivore molars, it does so for premolars (Figure 4b). Additionally, whereas OPCR does not differ significantly between the molars of folivores and frugivores, as well as between the molars of folivores and insectivores, premolar dental topography differs significantly between both those pairs (Figure 4c). The increase in classification accuracy when including both premolar and molar topography and size is because of these complementing patterns, which increase the differences between dietary categories.

5 | CONCLUSIONS

Dental topography metrics correlate to varying degrees between premolars and molars, but none do so very strongly (all with $r \leq 0.61$). Size however correlates very strongly between the two teeth. Complexity (OPCR) and size variance is greater for premolars than it is for molars, supporting a wider range of mastication functions for premolars, although this is not supported by their relatively low variance in curvature (ariaDNE).

Dental topography of premolars is able to successfully predict the diet of extant prosimians well (67.8% accurate). Compared to the classification accuracy of molars, premolar topography outperformed that of molars slightly. However, when a measure of size is included, premolars perform with similar accuracy as that of molars at predicting diet. The highest classification accuracies are reached when premolar and molar topography and size are included, and classification accuracy is comparable when premolar and molar variables are kept separate and when they are combined.

These findings support the hypothesis that premolar morphology reflects the functional requirements of a given dietary category in ways that are (1) consistent within but different between dietary categories and (2) are not already reflected by morphological variation in the molars. As a corollary, our results suggest that variation in molar morphology incompletely reflects variation in the functional requirements of a given dietary category, and that premolar morphology reflects some of the variance unexplained by molars. As such, we can conjecture that whereas molar morphology consistently reflects demands of the power stroke (or shearing–grinding phase) of mastication, premolar morphology does not. Most likely, the source of the selection pressure on premolars is more varied. In some taxa, it likely stems from ingestion and/or the puncture–crushing phase of chewing (found in our frugivore, omnivore, and, for some of the taxa in the insectivore dietary groups), whereas in others, namely folivores, it seems more likely to stem from the shearing–grinding phase, as it is for the molars. This variation in functional role can be explained by the spatially intermediate position of premolars between the anterior teeth, which are more involved in ingestion, and the molars, which are involved in both the puncture–crushing phase as well as the grinding phase of chewing.

In practical terms, our findings suggest fossil primate premolar specimens can be used for meaningful dietary reconstruction of extinct species in isolation, or (even better) in conjunction with fossil molars.

AUTHOR CONTRIBUTIONS

Dorien de Vries: Conceptualization (equal); data curation (lead); formal analysis (lead); methodology (equal); writing – original draft (lead); writing – review and editing (lead). **Julie M. Winchester:** Conceptualization (equal); methodology (equal); writing – review and editing (equal). **Ethan L. Fulwood:** Data curation (equal); methodology (equal); writing – review and editing (equal). **Elizabeth M. St. Clair:** Conceptualization (equal); funding acquisition (equal); methodology (equal); writing – review and editing (equal). **Doug M. Boyer:** Conceptualization (equal); funding acquisition (equal); methodology (equal); writing – review and editing (equal).

ACKNOWLEDGMENTS

DdeV was supported by funds from the Natural Environment Research Council (NERC, NE/T000341/1). Data collection was supported by funds from NSF (DBI-1759839, BCS-1552848, BCS-1304045) to DMB and ESC.

OPEN RESEARCH BADGES

This article has earned Open Data and Open Materials badges. Data and materials are available at https://osf.io/sbvr8/?view_only=2880aa60ff874717abc0bad05818c47f, https://www.morphosource.org/projects/000552618?locale=en.

DATA AVAILABILITY STATEMENT

Digital surface meshes of our study sample are openly available in MorphoSource at (https://www.morphosource.org/), project ID: 000552618. All R-code and input files can be found at: https://osf.io/sbvr8/?view_only=2880aa60ff874717abc0bad05818c47f.

ORCID

Dorien de Vries https://orcid.org/0000-0002-6809-0052
Elizabeth M. St. Clair https://orcid.org/0000-0002-2762-8944

REFERENCES

Allen, K. L., Cooke, S. B., Gonzales, L. A., & Kay, R. F. (2015). Dietary inference from upper and lower molar morphology in platyrrhine primates. *PLoS One*, *10*(3), e0118732. https://doi.org/10.1371/journal.pone.0118732

Arnold, C., Matthews, L. J., & Nunn, C. L. (2010). The 10kTrees website: A new online resource for primate phylogeny. *Evolutionary Anthropology*, *19*(3), 114–118. https://doi.org/10.1002/evan.20251

Avià, Y., Romero, A., Estebaranz-Sánchez, F., Pérez-Pérez, A., Cuesta-Torralvo, E., & Martínez, L. M. (2022). Dental topography and dietary specialization in Papionini primates. *Frontiers in Ecology and Evolution*, *10*, 969007. https://doi.org/10.3389/fevo.2022.969007

Berthaume, M. A., Delezene, L. K., & Kupczik, K. (2018). Dental topography and the diet of *Homo naledi*. *Journal of Human Evolution*, *118*, 14–26. https://doi.org/10.1016/j.jhevol.2018.02.006

Berthaume, M. A., & Schroer, K. (2017). Extant ape dental topography and its implications for reconstructing the emergence of early *Homo*. *Journal of Human Evolution*, *112*, 15–29. https://doi.org/10.1016/j.jhevol.2017.09.001

Berthaume, M. A., Winchester, J., & Kupczik, K. (2019a). Ambient occlusion and PCV (portion de ciel visible): A new dental topographic metric and proxy of morphological wear resistance. *PLoS One*, *14*(5), e0215436. https://doi.org/10.1371/journal.pone.0215436

Berthaume, M. A., Winchester, J., & Kupczik, K. (2019b). Effects of cropping, smoothing, triangle count, and mesh resolution on 6 dental topographic metrics. *PLoS One*, *14*(5), e0216229. https://doi.org/10.1371/journal.pone.0216229

Boyer, D. M. (2008). Relief index of second mandibular molars is a correlate of diet among prosimian primates and other euarchontan mammals. *Journal of Human Evolution*, *55*(6), 1118–1137. https://doi.org/10.1016/j.jhevol.2008.08.002

Boyer, D. M., Evans, A. R., & Jernvall, J. (2010). Evidence of dietary differentiation among late Paleocene-early Eocene plesiadapids (Mammalia, primates). *American Journal of Physical Anthropology*, *142*(2), 194–210. https://doi.org/10.1002/ajpa.21211

Boyer, D. M., Gunnell, G. F., Kaufman, S., & McGeary, T. M. (2016). MorphoSource: Archiving and sharing 3-D digital specimen data. *The Paleontological Society Papers*, *22*, 157–181. https://doi.org/10.1017/scs.2017.13

Bunn, J. M., Boyer, D. M., Lipman, Y., St. Clair, E. M., Jernvall, J., & Daubechies, I. (2011). Comparing Dirichlet normal surface energy of tooth crowns, a new technique of molar shape quantification for dietary inference, with previous methods in isolation and in combination. *American Journal of Physical Anthropology*, *145*(2), 247–261. https://doi.org/10.1002/ajpa.21489

Bunn, J. M., & Ungar, P. S. (2009). Dental topography and diets of four old world monkey species. *American Journal of Primatology*, *71*(6), 466–477. https://doi.org/10.1002/ajp.20676

Burrows, A. M., Nash, L. T., Hartstone-Rose, A., Silcox, M. T., López-Torres, S., & Selig, K. R. (2020). Dental signatures for exudativory in living primates, with comparisons to other gouging mammals. *Anatomical Record*, *303*(2), 265–281. https://doi.org/10.1002/ar.24048

Butler, P. (2000). The evolution of tooth shape and tooth function in primates. In M. F. Teaford, M. M. Smith, & M. W. Ferguson (Eds.), *Development, function and evolution of teeth* (pp. 201–212). Cambridge University Press.

Cabana, F., Dierenfeld, E., Wirdateti, W., Donati, G., & Nekaris, K. A. I. (2017). The seasonal feeding ecology of the javan slow loris (*Nycticebus javanicus*). *American Journal of Physical Anthropology*, *162*(4), 768–781. https://doi.org/10.1002/ajpa.23168

Cooke, S. B. (2011). Paleodiet of extinct platyrrhines with emphasis on the Caribbean forms: Three-dimensional geometric morphometrics of mandibular second molars. *Anatomical Record*, *294*(12), 2073–2091. https://doi.org/10.1002/ar.21502

Cuozzo, F. P., & Sauther, M. L. (2006). Severe wear and tooth loss in wild ring-tailed lemurs (*Lemur catta*): A function of feeding ecology, dental structure, and individual life history. *Journal of Human Evolution*, *51*(5), 490–505. https://doi.org/10.1016/j.jhevol.2006.07.001

Dammhahn, M., & Kappeler, P. M. (2008). Comparative feeding ecology of sympatric *Microcebus berthae* and *M. murinus*. *International Journal of Primatology*, *29*(6), 1567–1589. https://doi.org/10.1007/s10764-008-9312-3

De Vries, D., Janiak, M. C., Batista, R., Boubli, J. P., Goodhead, I. B., Ridgway, E., Boyer, D. M., St. Clair, E., & Beck, R. M. D. (2024). Comparison of dental topography of marmosets and tamarins (Callitrichidae) to other platyrrhine primates using a novel freeware pipeline. *Journal of Mammalian Evolution*, *31*(12), 1–20. https://doi.org/10.1007/s10914-024-09704-9

DeMers, A. C., & Hunter, J. P. (2024). Dental complexity and diet in amniotes: A meta-analysis. *PLoS One*, *19*(2), e0292358. https://doi.org/10.1371/journal.pone.0292358

Dennis, J. C., Ungar, P. S., Teaford, M. F., & Glander, K. E. (2004). Dental topography and molar wear in *Alouatta palliata* from Costa Rica. *American Journal of Physical Anthropology*, *125*(2), 152–161. https://doi.org/10.1002/ajpa.10379

Dinno, A., & Dinno, M. A. (2017). Package "dunn.test." https://cran.r-project.org/web/packages/dunn.test/index.html

Evans, A. R., & Jernvall, J. (2009). Patterns and constraints in carnivoran and rodent dental complexity and tooth size. *Journal of Vertebrate Paleontology*, *29*, 24A.

Evans, A. R., Wilson, G. P., Fortelius, M., & Jernvall, J. (2007). High-level similarity of dentitions in carnivorans and rodents. *Nature*, *445*(7123), 78–81. https://doi.org/10.1038/nature05433

Field, A., Miles, J., & Field, Z. (2012). *Discovering statistics using R* (pp. 1–992). SAGE Publications.

Fulwood, E. L., Shan, S., Winchester, J. M., Gao, T., Kirveslahti, H., Daubechies, I., & Boyer, D. M. (2021). Reconstructing dietary ecology of extinct strepsirrhines (primates, mammalia) with new approaches for characterizing and analyzing tooth shape. *Paleobiology*, *47*(4), 612–631. https://doi.org/10.1017/pab.2021.9

Godfrey, L. R., Winchester, J. M., King, S. J., Boyer, D. M., & Jernvall, J. (2012). Dental topography indicates ecological contraction of lemur communities. *American Journal of Physical Anthropology*, *148*(2), 215–227. https://doi.org/10.1002/ajpa.21615

Guy, F., Gouvard, F., Boistel, R., Euriat, A., & Lazzari, V. (2013). Prospective in (primate) dental analysis through tooth 3D topographical quantification. *PLoS One*, *8*(6), e66142. https://doi.org/10.1371/journal.pone.0066142

Hiiemae, K., & Kay, R. F. (1972). Trends in the evolution of primate mastication. *Nature*, *240*(5382), 486–487. https://doi.org/10.1038/240486a0

Hiiemae, K. M., & Crompton, A. W. (1985). Mastication, food transport, and swallowing. In M. Hildebrand, D. Bramble, K. Liem, & D. Wake (Eds.), *Functional vertebrate morphology* (pp. 262–290). Harvard University Press. https://doi.org/10.4159/harvard.9780674184404.c14

Kassambara, A. (2023). rstatix: pipe-friendly framework for basic statistical tests. R Package Version 0.7. 0. https://CRAN.R-project.org/package=rstatix

Kay, R. F. (1975). The functional adaptations of primate molar teeth. *American Journal of Physical Anthropology*, *43*(2), 195–216. https://doi.org/10.1002/ajpa.1330430207

Kay, R. F. (1978). Molar structure and diet in extant Cercopithecoidea. In P. M. Butler & K. Joysey (Eds.), *Development, function and evolution of teeth* (pp. 309–339). Academic Press.

Kay, R. F., & Hiiemae, K. M. (1974). Jaw movement and tooth use in recent and fossil primates. *American Journal of Physical Anthropology*, *40*(2), 227–256. https://doi.org/10.1002/ajpa.1330400210

Lahann, P. (2007). Feeding ecology and seed dispersal of sympatric Cheirogaleid lemurs (*Microcebus murinus*, *Cheirogaleus medius*, *Cheirogaleus major*) in the littoral rainforest of south-east Madagascar. *Journal of Zoology*, *271*(1), 88–98. https://doi.org/10.1111/j.1469-7998.2006.00222.x

Lazzari, V., & Guy, F. (2014). Quantitative three-dimensional topography in taxonomy applied to the dental morphology of catarrhines. *BMSAP*, *26*(3), 140–146. https://doi.org/10.1007/s13219-014-0099-9

Li, P., Morse, P. E., & Kay, R. F. (2020). Dental topographic change with macrowear and dietary inference in *Homunculus patagonicus*. *Journal of Human Evolution*, *144*, 102786.

Long, C., Tordiffe, A., Sauther, M., Cuozzo, F., Millette, J., Ganswindt, A., & Scheun, J. (2021). Seasonal drivers of faecal glucocorticoid metabolite concentrations in an African strepsirrhine primate, the thick-tailed greater galago (*Otolemur crassicaudatus*). *Conservation Physiology*, *9*(1), coab081. https://doi.org/10.1093/conphys/coab081

López-Torres, S., Selig, K. R., Prufrock, K. A., Lin, D., & Silcox, M. T. (2018). Dental topographic analysis of paromomyid (Plesiadapiformes, primates) cheek teeth: More than 15 million years of changing surfaces and shifting ecologies. *Historical Biology*, *30*(1–2), 76–88. https://doi.org/10.1080/08912963.2017.1289378

Maier, W. (1984). Tooth morphology and dietary specialization. In D. J. Chivers, B. A. Wood, & A. Bilsborough (Eds.), *Food acquisition and processing in primates* (pp. 303–330). Springer US. https://doi.org/10.1007/978-1-4757-5244-1_13

Matlab, Version: 9 11 0 r2021b. (2021). The MathWorks Inc., Natick, MA, USA.

Melstrom, K. M. (2017). The relationship between diet and tooth complexity in living dentigerous saurians. *Journal of Morphology*, *278*(4), 500–522. https://doi.org/10.1002/jmor.20645

Melstrom, K. M., & Irmis, R. B. (2019). Repeated evolution of herbivorous crocodyliforms during the age of dinosaurs. *Current Biology: CB*, *29* (14), 2389–2395.e3. https://doi.org/10.1016/j.cub.2019.05.076

M'Kirera, F., & Ungar, P. S. (2003). Occlusal relief changes with molar wear in *Pan troglodytes troglodytes* and *Gorilla gorilla gorilla*. *American Journal of Primatology*, *60*(2), 31–41. https://doi.org/10.1002/ajp.10077

Morse, P. E., Pampush, J. D., & Kay, R. F. (2023). Dental topography of the Oligocene anthropoids *Aegyptopithecus zeuxis* and *Apidium phiomense*: Paleodietary insights from analysis of wear series. *Journal of Human Evolution*, *180*, 103387. https://doi.org/10.1016/j.jhevol.2023.103387

Orme, D., Freckleton, R., Thomas, G., Petzoldt, T., Fritz, S., Isaac, N., Pearse, W., & Orme, M. D. (2018). Package "caper." R Cran, 1–50. https://cran.gedik.edu.tr/web/packages/caper/caper.pdf

Pampush, J. D., Morse, P. E., Fuselier, E. J., Skinner, M. M., & Kay, R. F. (2022). Sign-oriented Dirichlet normal energy: Aligning dental topography and dental function in the R-package molaR. *Journal of Mammalian Evolution*, *29*, 713–732. https://doi.org/10.1007/s10914-022-09616-6

Pampush, J. D., Spradley, J. P., Morse, P. E., Harrington, A. R., Allen, K. L., Boyer, D. M., & Kay, R. F. (2016). Wear and its effects on dental topography measures in howling monkeys (*Alouatta palliata*). *American Journal of Physical Anthropology*, *161*(4), 705–721. https://doi.org/10.1002/ajpa.23077

Pampush, J. D., Winchester, J. M., Morse, P. E., Vining, A. Q., Boyer, D. M., & Kay, R. F. (2016). Introducing molaR: A new R package for quantitative topographic analysis of teeth (and other topographic surfaces). *Journal of Mammalian Evolution*, *23*, 397–412. https://doi.org/10.1007/s10914-016-9326-0

Prufrock, K. A., Boyer, D. M., & Silcox, M. T. (2016). The first major primate extinction: An evaluation of paleoecological dynamics of north American stem primates using a homology free measure of tooth shape. *American Journal of Physical Anthropology*, *159*(4), 683–697. https://doi.org/10.1002/ajpa.22927

R Core Team. (2022). *R: A language and environment for statistical computing*. R Foundation for Statistical Computing. https://www.R-project.org/

Revell, L. J. (2012). Phytools: An R package for phylogenetic comparative biology (and other things). *Methods in Ecology and Evolution/British Ecological Society*, *3*(2), 217–223. https://doi.org/10.1111/j.2041-210x.2011.00169.x

Ripley, B., Venables, B., Bates, D. M., Hornik, K., Gebhardt, A., Firth, D., & Ripley, M. B. (2013). *Package "mass."*. https://cran.r-project.org/web/packages/MASS/index.html

Rode-Margono, E. J., Nijman, V., Wirdateti, N. K., & Nekaris, K. A. I. (2014). Ethology of the critically endangered Javan slow loris *Nycticebus javanicus* E. Geoffroy saint-Hilaire in West Java. *Asian Primates*, *4*(2), 27–38.

Santana, S. E., Strait, S., & Dumont, E. R. (2011). The better to eat you with: Functional correlates of tooth structure in bats. *Functional Ecology*, *25*(4), 839–847. https://doi.org/10.1111/j.1365-2435.2011.01832.x

Scott, J. E., Campbell, R. M., Baj, L. M., Burns, M. C., Price, M. S., Sykes, J. D., & Vinyard, C. J. (2018). Dietary signals in the premolar dentition of primates. *Journal of Human Evolution*, *121*, 221–234. https://doi.org/10.1016/j.jhevol.2018.04.006

Seiffert, E. R., Boyer, D. M., Fleagle, J. G., Gunnell, G. F., Heesy, C. P., Perry, J. M. G., & Sallam, H. M. (2018). New adapiform primate fossils from the late Eocene of Egypt. *Historical Biology*, *30*(1–2), 204–226. https://doi.org/10.1080/08912963.2017.1306522

Seiffert, E. R., Costeur, L., & Boyer, D. M. (2015). Primate tarsal bones from Egerkingen, Switzerland, attributable to the middle Eocene adapiform *Caenopithecus lemuroides*. *PeerJ*, *3*, e1036. https://doi.org/10.7717/peerj.1036

Seiffert, E. R., Simons, E. L., Boyer, D. M., Perry, J. M. G., Ryan, T. M., & Sallam, H. M. (2010). A fossil primate of uncertain affinities from the earliest late Eocene of Egypt. *Proceedings of the National Academy of Sciences of the United States of America*, *107*(21), 9712–9717. https://doi.org/10.1073/pnas.1001393107

Selig, K. R., Chew, A. E., & Silcox, M. T. (2021). Dietary shifts in a group of early *Eocene euarchontans* (Microsyopidae) in association with climatic change. *Palaeontology*, *64*(5), 609–628.

Selig, K. R., Schroeder, L., & Silcox, M. T. (2021). Intraspecific variation in molar topography of the early Eocene stem primate *Microsyops latidens* (Mammalia, ? Primates). *Journal of Vertebrate Paleontology*, *41*(4), e1995738. https://doi.org/10.1080/02724634.2021.1995738

Selig, K. R., & Silcox, M. T. (2022). Measuring molarization: Change through time in premolar function in an extinct stem primate lineage. *Journal of Mammalian Evolution*, *29*(4), 947–956. https://doi.org/10.1007/s10914-022-09623-7

Seligsohn, D., & Szalay, F. S. (1978). Relationship between natural selection and dental morphology: Tooth function and diet in *Lepilemur*. In P. M. Butler & A. Joysey (Eds.), *Development, function and evolution of teeth* (pp. 289–307). London.

Shan, S., Kovalsky, S. Z., & Winchester, J. M. (2019). ariaDNE: A robustly implemented algorithm for Dirichlet energy of the normal. *Methods in Ecology and Evolution/British Ecological Society*, *10*, 541–552. https://doi.org/10.1111/2041-210X.13148

Simpson, G. G. (1933). Paleobiology of jurassic mammals. In *Palaeobiologica* (Vol. 5, pp. 127–158). Emil Haim & Co.

Spradley, J. P., Pampush, J. D., Morse, P. E., & Kay, R. F. (2017). Smooth operator: The effects of different 3D mesh retriangulation protocols on the computation of Dirichlet normal energy. *American Journal of Physical Anthropology*, *163*(1), 94–109. https://doi.org/10.1002/ajpa.23188

Strait, S. G. (1993a). Differences in occlusal morphology and molar size in frugivores and faunivores. *Journal of Human Evolution*, *25*(6), 471–484. https://doi.org/10.1006/jhev.1993.1062

Strait, S. G. (1993b). Molar morphology and food texture among small-bodied insectivorous mammals. *Journal of Mammalogy*, *74*(2), 391–402. https://doi.org/10.2307/1382395

Swindler, D. R. (2002). *Primate dentition: An introduction to the teeth of non-human primates*. Cambridge University Press. https://doi.org/10.1017/CBO9780511542541

Thorén, S., Quietzsch, F., Schwochow, D., Sehen, L., Meusel, C., Meares, K., & Radespiel, U. (2011). Seasonal changes in feeding ecology and activity patterns of two sympatric mouse lemur species, the gray mouse lemur (*Microcebus murinus*) and the golden-brown mouse lemur (*M. ravelobensis*), in northwestern Madagascar. *International Journal of Primatology*, *32*(3), 566–586. https://doi.org/10.1007/s10764-010-9488-1

Tiphaine, C., Yaowalak, C., Cyril, C., Helder, G.-R., Jacques, M., Paul, T., Monique, V.-L., Laurent, V., & Vincent, L. (2013). Correlated changes in occlusal pattern and diet in stem Murinae during the onset of the radiation of old world rats and mice. *Evolution; International Journal of Organic Evolution*, *67*(11), 3323–3338. https://doi.org/10.1111/evo.12172

Ungar, P. S. (2004). Dental topography and diets of *Australopithecus afarensis* and early *Homo*. *Journal of Human Evolution*, *46*(5), 605–622. https://doi.org/10.1016/j.jhevol.2004.03.004

Ungar, P. S., Healy, C., Karme, A., Teaford, M., & Fortelius, M. (2018). Dental topography and diets of platyrrhine primates. *Historical Biology*, *30* (1–2), 64–75. https://doi.org/10.1080/08912963.2016.1255737

Ungar, P. S., & M'Kirera, F. (2003). A solution to the worn tooth conundrum in primate functional anatomy. *Proceedings of the National*

Academy of Sciences of the United States of America, *100*(7), 3874–3877. https://doi.org/10.1073/pnas.0637016100

Ungar, P. S., & Williamson, M. (2000). Exploring the effects of tooth wear on functional morphology: A preliminary study using dental topographic analysis. *Palaeontologia Electronica*, *3*(1), 1–18.

Winchester, J. M. (2016a). *Molar topographic shape as a system for inferring functional morphology and developmental patterning in extant Cercopithecoid primates (unpublished doctoral dissertation)*. State University of New York, Stony Brook.

Winchester, J. M. (2016b). MorphoTester: An open source application for morphological topographic analysis. *PLoS One*, *11*(2), e0147649. https://doi.org/10.1371/journal.pone.0147649

Winchester, J. M., Boyer, D. M., St Clair, E. M., Gosselin-Ildari, A. D., Cooke, S. B., & Ledogar, J. A. (2014). Dental topography of platyrrhines and prosimians: Convergence and contrasts. *American Journal of Physical Anthropology*, *153*(1), 29–44. https://doi.org/10.1002/ajpa.22398

Zuccotti, L. F., Williamson, M. D., Limp, W. F., & Ungar, P. S. (1998). Technical note: Modeling primate occlusal topography using geographic information systems technology. *American Journal of Physical Anthropology*, *107*(1), 137–142. https://doi.org/10.1002/(SICI)1096-8644(199809)107:1<137::AID-AJPA11>3.0.CO;2-1

SUPPORTING INFORMATION

Additional supporting information can be found online in the Supporting Information section at the end of this article.

How to cite this article: de Vries, D., Winchester, J. M., Fulwood, E. L., St. Clair, E. M., & Boyer, D. M. (2024). Dental topography of prosimian premolars predicts diet: A comparison in premolar and molar dietary classification accuracies. *American Journal of Biological Anthropology*, e24995. https://doi.org/10.1002/ajpa.24995